General series solution for finite square-well energy levels for use in wave-packet studies

David L. Aronstein[a] and C. R. Stroud, Jr.
The Institute of Optics, University of Rochester, Rochester, New York 14627

(Received 23 July 1999; accepted 11 January 2000)

We develop a series solution for the bound-state energy levels of the quantum-mechanical one-dimensional finite square-well potential. We show that this general solution is useful for *local* approximations of the energy spectrum (which target a particular energy range of the potential well for high accuracy), for *global* approximations of the energy spectrum (which provide analytic expressions of reasonable accuracy for the entire range of bound states), and for numerical methods. This solution also provides an analytic description of dynamical phenomena; with it, we compute the time scales of classical motion, revivals, and super-revivals for wave-packet states excited in the well. © *2000 American Association of Physics Teachers.*

I. INTRODUCTION

The study of a particle confined to a one-dimensional box of finite depth (called ''one of the workhorse problems of elementary quantum mechanics'' by Cantrell[1]) is important both to physics education and to simple models of realistic potentials. It challenges students of quantum mechanics to connect a confining potential with issues of boundary conditions, wave-function continuity, and energy quantization, and motivates the need for finding approximate solutions to equations (in this case, transcendental) that do not have closed-form answers. Excellent elementary treatments of this system are found in popular textbooks.[2–5]

Introductory quantum mechanics courses often focus on problems of *structure*, determining the energy levels and eigenfunctions for various one-dimensional potentials. It seems under-appreciated that these can be taught naturally in conjunction with problems of *dynamics*: When a particle is prepared in a spatially localized wave packet instead of in an energy eigenstate, it initially exhibits *classical motion*,[6] moving back and forth periodically in the potential well. During this periodic motion, however, the wave packet slowly spreads out and decays away. Long after this decay, there are windows of time, called *revivals* and *super-revivals*, during which the packet and its classical behavior briefly reappear. Although the mathematical description of these phenomena may be beyond the scope of an introductory course, we believe that studying wave packets helps students understand the connections between classical and quantum mechanics and strengthens their intuition for the quantum physics.

A deep knowledge of the structure of a quantum-mechanical potential is the most important tool for understanding its dynamics. The wave-packet time scales for classical motion, revivals, and super-revivals are related to derivatives of the energy spectrum[7,8] and are readily determined in systems such as the simple harmonic oscillator,[9] the hydrogen atom,[10] or the infinite square-well potential,[11] in which the energy levels have simple analytic form. These times have not been derived for the finite square-well potential because of the transcendental nature of the equations describing the energy spectrum. In the present paper we show that a series solution for the energies is the necessary tool to determine these time scales, to connect the structure and dynamics in the finite well in a way that is impossible when only the numerical values of energy are known.

In Sec. III, we develop a general series solution for the energy spectrum that makes use of a ''height ratio'' r, allowing the solution to be ''tuned'' to different energy ranges in the well. This can be used in problems of structure in three different ways: (a) As *local* approximations of the energy spectrum (Sec. IV), which target a particular energy range of the potential well for highest accuracy. Series solutions for the spectrum at the bottom and in the middle of the well are given as examples. These local approximations provide high accuracy with relatively simple expressions, but different approximations are needed for each energy range of interest. (b) As *global* approximations of the energy spectrum (Sec. V A) which describe the full spectrum of the well and are judged by their ''worst-case'' error (the largest percentage error predicted, for all energy levels and potential well depths). These global approximations converge rapidly throughout the well but describe a rather complicated dependence on the quantum number. (c) As *numerical methods* for evaluating the energy levels (Sec. V B), which provide higher-order (and faster-converging) generalizations of the familiar Newton–Raphson root-finding method.

In Sec. VI, we turn to problems of dynamics. We use the general series solution to predict the time scales for classical motion, revivals, and super-revivals of wave-packet states excited in the finite square-well potential and show an example of the wave-packet motion described by these times.

II. ENERGY QUANTIZATION EQUATION

The finite square-well potential in quantum mechanics confines a nonrelativistic particle of mass m to a box of length L and potential depth V_0 and is described by

$$V(x)=\begin{cases}0, & |x|\leqslant L/2,\\ V_0, & |x|>L/2.\end{cases} \tag{1}$$

The discrete bound-state energy eigenfunctions (with energy $0<E<V_0$) are found by solving the time-independent Schrödinger equation in each region of constant potential separately. These eigenfunctions are superpositions of left- and right-traveling waves inside the well and attenuating waves outside and are written in the form

$$\psi_n(x)=\begin{cases} A_- \exp[-\sqrt{2m(V_0-E)}|x|/\hbar], & x<-L/2, \\ T_+ \exp[+i\sqrt{2mE}x/\hbar] & \\ \quad +T_- \exp[-i\sqrt{2mE}x/\hbar], & |x|\leqslant L/2, \\ A_+ \exp[-\sqrt{2m(V_0-E)}|x|/\hbar], & x>L/2, \end{cases} \tag{2}$$

with unknown coefficients $A_\pm$ and $T_\pm$. This suggests two useful dimensionless quantities (using notation from Barker *et al.*[12]): The *scaled action* α depends on the particle energy E with

$$\alpha=\frac{\sqrt{2mE}}{\hbar}\frac{L}{2}, \tag{3}$$

and the *well-strength parameter* P depends on the potential depth V_0 with

$$P=\frac{\sqrt{2mV_0}}{\hbar}\frac{L}{2}. \tag{4}$$

The conditions for the quantization of the stationary energies supported by the square well are found by examining the continuity of the wave functions $\psi_n(x)$ and their spatial derivatives $\psi_n'(x)$ at the well boundaries ($x=\pm L/2$). The energy eigenstates manifest the symmetry of the potential and are states of definite parity. Many quantum mechanics textbooks[2–5] study even-parity states (with $A_-=A_+$ and $T_-=T_+$) separately from odd-parity states (with $A_-=-A_+$ and $T_-=-T_+$) to simplify the mathematical analysis and find that the quantization conditions for the energy levels are

$$\begin{aligned} &\alpha\tan\alpha=\sqrt{P^2-\alpha^2}, && \text{even parity,} \\ &\alpha\cot\alpha=-\sqrt{P^2-\alpha^2}, && \text{odd parity.} \end{aligned} \tag{5}$$

Cantrell[1] showed that these can be simplified substantially, at the expense of introducing sign ambiguity, to

$$\begin{aligned} &\cos\alpha=\pm\frac{\alpha}{P}, && \text{even parity,} \\ &\sin\alpha=\pm\frac{\alpha}{P}, && \text{odd parity.} \end{aligned} \tag{6}$$

Equations (5) and (6) are often solved by students using graphical methods. The physics literature has a long tradition of using geometrical constructions to determine square-well energy levels, including finding the intersection of circles[13] or straight lines[1,14] with trigonometric functions, using absolute values to clarify the sign ambiguities,[15,16] or making plots in polar coordinates.[17] Burge further showed[18] that the eigenstates $\psi_n(x)$ and probability densities $|\psi_n(x)|^2$ can be constructed graphically.

Equations (5) and (6), separated by parity, are not ideal for our purposes. Instead, it is useful to find a unified equation describing all the energy levels. Without dividing states by parity, Reed showed[19] that the quantization condition is

$$\left(1-2\frac{\alpha^2}{P^2}\right)\sin 2\alpha+\left(2\frac{\alpha}{P}\sqrt{1-\frac{\alpha^2}{P^2}}\right)\cos 2\alpha=0 \tag{7}$$

and demonstrated graphical solutions of this equation. Sprung, Wu, and Martorell[20] observed that this is an identity for the sine of the sum of two angles,

$$\sin[2(\alpha+\Phi)]=0, \tag{8}$$

where angle Φ is given by

$$\Phi=\sin^{-1}\left(\frac{\alpha}{P}\right). \tag{9}$$

With Eqs. (8) and (9), they found a beautiful and remarkably simple expression for the quantization condition, that the bound-state energies are solutions of the equation

$$\alpha+\sin^{-1}\left(\frac{\alpha}{P}\right)=\frac{n\pi}{2}, \tag{10}$$

which relates the scaled action α to the quantum number n for a given well-strength parameter P. The importance of Eq. (10) over its predecessors is the explicit appearance of the quantum number. With this, for example, the nth energy level can be determined directly without first needing to find the preceding $n-1$ quantized solutions.

Note that we choose the branch $-\pi/2\leqslant\sin^{-1}(\alpha/P)\leqslant\pi/2$ of the arcsine function in Eq. (10), and with this the ground state (the lowest positive solution α) corresponds to quantum number $n=1$.

A. Semiclassical interpretation

Here we offer a physical interpretation for the quantization condition, Eq. (10), using insights gained from semiclassical quantum mechanics. We consider a particle with momentum p_x, with which we associate a de Broglie wave with wave number $k=p_x/\hbar$ and wavelength $\lambda=2\pi/k$. Inside the finite square-well potential, the particle is described as traveling back and forth, colliding with and bouncing off the well boundaries, whereas the corresponding de Broglie wave is described as reflecting at the well edges from the discontinuity in the potential.

After completing one round trip (of length $2L$) inside the well, the de Broglie wave will have experienced a phase change of $2kL$ from its propagation and a phase shift of ϕ from reflection at each boundary of the well. In a semiclassical analysis, we expect the total phase change experienced by an energy eigenstate to be a multiple of 2π, that the eigenstate has constructive interference after one round trip and forms a standing-wave pattern inside the well. The total phase change then satisfies

$$2kL+2\phi=2\pi n, \tag{11}$$

for integer n. The left- and right-traveling waves inside the well can be described with ''plane-wave'' exponentials $\exp[\pm ikx]$, thus with Eq. (2) we anticipate that the wave number is given by

$$k=\frac{\sqrt{2mE}}{\hbar}=\frac{2\alpha}{L}. \tag{12}$$

With this, the semiclassical quantization condition becomes

$$\alpha+\frac{\phi}{2}=\frac{n\pi}{2}. \tag{13}$$

This agrees with the rigorously derived quantization equation (10) if we take

$$\frac{\phi}{2}=\Phi=\sin^{-1}\left(\frac{\alpha}{P}\right). \tag{14}$$

Physically, $\phi = 2\sin^{-1}(\alpha/P)$ is the phase shift experienced on reflection at the finite square-well boundary, or equivalently, the extra phase accumulated from penetrating beyond the boundary.

III. GENERAL SERIES SOLUTION OF THE ENERGY SPECTRUM

The quantization condition (10) is a transcendental equation for α. In order to determine the energy spectrum, this must be transformed into an invertible equation. We do this by focusing on a particular energy region of the well; this region of interest is specified by a height ratio r $(0 \leqslant r \leqslant 1)$, describing the well bottom with $r=0$ and the well top with $r=1$. With a Taylor series of the boundary reflection phase Φ in the vicinity of this height ratio $(\alpha/P = r)$, the quantization condition becomes

$$\alpha + \left[\sin^{-1} r + \frac{1}{\sqrt{1-r^2}}\left(\frac{\alpha}{P} - r\right) + \frac{r}{2(1-r^2)^{3/2}}\left(\frac{\alpha}{P} - r\right)^2 + \frac{1+2r^2}{6(1-r^2)^{5/2}}\left(\frac{\alpha}{P} - r\right)^3 + \cdots \right] = \frac{n\pi}{2}. \tag{15}$$

This relates the quantum number n to a power series in the quantity $(\alpha/P - r)$. We invert this equation using the power series inversion theorem,[21,22] allowing us to describe $(\alpha/P - r)$ as a power series in quantity $\eta = (n\pi/2 - \sin^{-1} r - rP)$. Solving for α, we find

$$\alpha = P\left[r + \frac{P\sqrt{1-r^2}}{(1+P\sqrt{1-r^2})}\,\eta - \frac{rP}{2(1+P\sqrt{1-r^2})^3}\,\eta^2 - \frac{P^2(1+2r^2)+P\sqrt{1-r^2}}{6(1+P\sqrt{1-r^2})^5}\,\eta^3 - \cdots \right]. \tag{16}$$

With Eq. (3) this gives an energy spectrum (in units of $\hbar^2/mL^2$) of

$$E = 2P^2\left[r^2 + \frac{2r\sqrt{1-r^2}}{(1+P\sqrt{1-r^2})}\,\eta + \frac{(1-r^2)(1+P\sqrt{1-r^2})-r^2}{(1+P\sqrt{1-r^2})^3}\,\eta^2 - \frac{rP(4-r^2)+4r\sqrt{1-r^2}}{3(1+P\sqrt{1-r^2})^5}\,\eta^3 + \cdots \right]. \tag{17}$$

The function $\sin^{-1}(\alpha/P)$ has a logarithmic branch point at $\alpha/P = 1$, thus the analytic expansion in Eq. (15) and the predicted spectrum (17) are valid only for $2r-1 \leqslant \alpha/P \leqslant 1$. In principle, for $0 \leqslant r \leqslant 1/2$ the series converges for all energy levels in the square well, but in practice, few-term truncations of Eq. (17) are only useful in small neighborhoods around $\alpha/P = r$. For $r > 1/2$ we lose the ability to predict the spectrum at the bottom of the well, and as $r \to 1$ the expansion in Eq. (15) diverges and the region of convergence of Eq. (17) shrinks to zero. A robust description of the energy spectrum at the top of the well, using a nonpolynomial function that shares the arcsine's singularity, was developed by Sprung, Wu, and Martorell[20,23] to describe the scattering of continuum wave packets excited above the well.

The series solution (17) is the centerpiece of this paper. In the following sections, we show its use in *local* and *global* approximations of the finite square-well energy spectrum, in numerical methods, and in predicting the time scales important to revival phenomena of dynamical wave packets excited in the well.

IV. LOCAL APPROXIMATIONS

With a *fixed* value of the height ratio r, the general series solution (17) serves as a *local* approximation of the energy spectrum, in which a particular energy range of the well is targeted for highest accuracy. Here we show two examples.

A. Bottom of the well

The bottom of the well is described with height ratio $r=0$. The energy spectrum at the well bottom (in units of $\hbar^2/mL^2$) is found with Eq. (17) to be

$$E_n = \frac{2P^2}{(P+1)^2}\left[\left(\frac{n\pi}{2}\right)^2 - \frac{1}{3(P+1)^3}\left(\frac{n\pi}{2}\right)^4 - \frac{27P-8}{180(P+1)^6}\left(\frac{n\pi}{2}\right)^6 - \cdots \right]. \tag{18}$$

This region of the well is important because it describes the behavior in the infinite square-well limit: For an infinitely deep potential well $(P \to \infty)$, Eq. (18) reduces to the well-known result

$$\lim_{P\to\infty} E_n = \frac{\pi^2\hbar^2}{2mL^2}\,n^2. \tag{19}$$

Equation (18) also gives the leading-order correction factor $P^2/(P+1)^2$ that distinguishes the low-lying states of a finite well from those in an infinite square well.

Numerical tests of Eq. (18), comparing its results with numerical solutions of the exact quantization equation for various values of the well-strength parameter P, are presented in Table I. The exact numerical solutions cited in this paper were computed using the second-order iteration scheme described in Sec. V B.

The spectrum (18) has been computed elsewhere: The first term was calculated by Cantrell[1] for the closely related problem of the semi-infinite square well (an infinite potential boundary on one side and a finite boundary on the other). Barker *et al.*[12] found the first two terms using the parity-separated quantization conditions, Eq. (6). Sprung, Wu, and Martorell[20] derived this in full. Our contribution is to show that this follows immediately from the general series solution (17).

B. Middle of the well

The middle of the well is described with height ratio $r=1/2$. The energy spectrum in this region is described as a power series in the quantity $\eta = (n\pi/2 - \pi/6 - P/2)$ and (in units of $\hbar^2/mL^2$) is found to be

$$E_\eta = P^2\left[\frac{1}{2} + \frac{6}{(3P+2\sqrt{3})}\,\eta + \frac{6(9P+4\sqrt{3})}{(3P+2\sqrt{3})^3}\,\eta^2 - \frac{72(5\sqrt{3}P+8)}{(3P+2\sqrt{3})^5}\,\eta^3 + \cdots \right]. \tag{20}$$

Table I. Bottom of the well: Numerical tests comparing the exact energy levels (in units of $\hbar^2/mL^2$) to the second-, fourth-, and sixth-order truncations of Eq. (18). Values in parentheses are the percentage error between exact and approximated energies.

P	Exact energy	Second order	Fourth order	Sixth order
1.00	1.0925	1.2337	1.1069	1.0945
		(12.93%)	(1.32%)	(0.18%)
4.50	3.2867	3.3035	3.2871	3.2867
		(0.51%)	(0.01%)	(<0.01%)
	12.9179	13.2139	12.9526	12.9232
		(2.29%)	(0.27%)	(0.04%)
	27.8821	29.7312	28.4084	28.0744
		(6.63%)	(1.89%)	(0.69%)
6.00	3.6167	3.6256	3.6169	3.6167
		(0.24%)	(<0.01%)	(<0.01%)
	14.3518	14.5023	14.3632	14.3529
		(1.05%)	(0.08%)	(<0.01%)
	31.7736	32.6301	31.9259	31.8089
		(2.70%)	(0.48%)	(0.11%)
	54.6214	58.0091	55.7835	55.1261
		(6.20%)	(2.13%)	(0.92%)

Table II. Middle of the well: Numerical tests comparing the exact energy levels (in units of $\hbar^2/mL^2$) to the first-, second-, and third-order truncations of Eq. (20).

P	Exact energy	First order	Second order	Third order
1.00	1.0925	1.0079	1.1139	1.0964
		(7.74%)	(1.96%)	(0.36%)
4.50	3.2867	1.5103	3.2180	3.3028
		(54.05%)	(2.09%)	(0.49%)
	12.9179	12.7606	12.9205	12.9181
		(1.22%)	(0.02%)	(<0.01%)
	27.8821	24.0110	28.4479	28.0927
		(13.88%)	(2.03%)	(0.76%)
6.00	3.6167	−1.6517	3.4235	3.6776
		(145.67%)	(5.34%)	(1.68%)
	14.3518	14.1558	14.3500	14.3519
		(1.37%)	(0.01%)	(<0.01%)
	31.7736	29.9632	31.8440	31.7867
		(5.70%)	(0.22%)	(0.04%)
	54.6214	45.7706	55.9055	55.1886
		(16.20%)	(2.35%)	(1.04%)

The middle of the well is important as a model for the spectrum when the eigenstates extend appreciably outside of the well and when the effect of the boundary-reflection phase Φ plays a more significant role. Numerical tests of Eq. (20) are presented in Table II.

The local approximations offer a systematic way to describe a range of energy levels in the finite square well with a series solution. They converge to the exact energy levels, and truncations of the series are valuable as simple analytic models of the energy spectrum in the region of interest. The key trade-off with the local approximations is that they perform poorly outside the targeted energy range.

V. GLOBAL APPROXIMATIONS AND NUMERICAL METHODS

With a *variable* value of the height ratio r (that changes with quantum number), the general solution serves as a *global* approximation of the energy spectrum, which is accurate throughout the well and does not deliberately target one area of the well at the expense of results elsewhere. We show one scheme for implementing such a global approximation and connect this with numerical methods for determining the energy levels.

A. Global approximations

The general series solution becomes useful as a global approximation method if we estimate how the height ratio r varies with quantum number n and well strength P. We find that a good ''rule of thumb'' is to choose

$$r(n,P)=\frac{1}{P+\pi/2}\,\frac{n\pi}{2}. \tag{21}$$

This is motivated by the following observations: (a) Choosing $r\propto n$ can be argued from the leading-order approximation at the bottom of the well, Eq. (18), which predicts $r=\alpha/P=(P+1)^{-1}(n\pi/2)$. This estimate should be lowered slightly, as it predicts $r>1$ for some weakly bound states. (b) A finite well only supports a fixed number of bound states, given by

$$n_{\max}=\mathrm{int}\left(\frac{P}{\pi/2}\right)+1 \tag{22}$$

[with int(x) equal to the largest integer smaller than x], so our choice of height ratio r follows the ratio $n/n_{\max}$ if the integer truncation in Eq. (22) were removed. Thus the ratio in Eq. (21) always satisfies $0<r\leqslant 1$, and we have confirmed numerically that this height ratio r and the true scaled energy α always satisfy $2r-1\leqslant\alpha/P\leqslant 1$, the necessary criterion for uniform convergence. (c) Removing the integer truncation in the ratio $r=n/n_{\max}$ lowers the estimated values of r. In Sec. III, we noted that underestimating r, avoiding the limit $r\to 1$ when possible, gives a more generous region of convergence for the series solution.

The combination of Eqs. (17) and (21) is a highly effective method for determining the energy levels. Truncating the expansion to first order predicts all energy levels with $<5.56\%$ error. The second-order solution is accurate to $<1.57\%$ error, and the third-order expression provides $<0.11\%$ error. Numerical examples of this are given in Table III.

The global approximations show that it is possible to give highly accurate descriptions of the entire finite square-well energy spectrum. They converge rapidly, but we find that they are best used when it is not necessary to interpret the analytical form of the approximations, since the dependence on the quantum number (found both in the quantities η and r) is quite complicated.

B. Numerical iteration

If we knew $r=\alpha/P$ *a priori* for a particular energy level, then we would also know the scaled action $\alpha=rP$ and the energy $E=2r^2P^2(\hbar^2/mL^2)$ exactly; that is why these quantities appear as the leading terms in Eqs. (16) and (17), respectively. The higher-order terms in these equations are then understood as corrections needed for an inaccurate

Table III. Global approximation: Numerical tests comparing the exact energy levels (in units of $\hbar^2/mL^2$) to the first-, second-, and third-order truncations of Eq. (17) seeded with Eq. (21). For each approximation, the global worst-case error is provided, found numerically by testing the approximation at all quantum numbers for a wide range of well-strength parameters.

P	Exact energy	First order	Second order	Third order
1.00	1.0925	1.0733	1.0971	1.0930
		(1.76%)	(0.42%)	(0.04%)
4.50	3.2867	3.2594	3.2867	3.2867
		(0.83%)	(<0.01%)	(<0.01%)
	12.9179	12.8347	12.9190	12.9179
		(0.64%)	(<0.01%)	(<0.01%)
	27.8821	27.8189	27.8912	27.8831
		(0.23%)	(0.03%)	(<0.01%)
6.00	3.6167	3.5969	3.6167	3.6167
		(0.55%)	(<0.01%)	(<0.01%)
	14.3518	14.2827	14.3520	14.3518
		(0.48%)	(<0.01%)	(<0.01%)
	31.7736	31.6624	31.7755	31.7737
		(0.35%)	(<0.01%)	(<0.01%)
	54.6214	54.5710	54.6323	54.6226
		(0.09%)	(0.02%)	(<0.01%)
Worst-case error		$P\approx 0.155$ $n=1$	$P\approx 0.319$ $n=1$	$P\approx 0.506$ $n=1$
		(5.56%)	(1.57%)	(0.11%)

choice of r. This suggests an interpretation of the general series solution as a scheme for numerical iteration.

An initial choice for r [seeded, for example, using Eq. (21)] can be used in a few-term truncation of Eq. (16) to estimate α numerically. Then $r=\alpha/P$ is recomputed and this procedure is iterated until the expansion variable η becomes arbitrarily close to zero. Using the first-order truncation of Eq. (16) is precisely the Newton–Raphson root-finding method[24] for determining the energy, but here we also provide higher-order (and faster-converging) methods.

VI. WAVE-PACKET REVIVAL PHENOMENA

Our motivation for developing the general series solution (17) was to aid our study of wave-packet states excited in the finite square well. In this section, we show how the general series solution provides analytic expressions for the time scales important in wave-packet dynamics.

A. Wave-packet revival times

We consider a wave-packet state excited in the square well, in which the particle's wave function is a coherent superposition of bound energy levels centered around mean quantum number $\overline{n}$. It has been shown[7,8] that the important time scales for the wave-packet's dynamics are given in terms of derivatives of the energy spectrum E_n in the vicinity of the wave-packet's mean quantum number $\overline{n}$. Specifically, the time scales

$$T_1=\frac{2\pi\hbar}{|E_{\overline{n}}'|},\quad T_2=\frac{2\pi\hbar}{|E_{\overline{n}}''|},\quad T_3=\frac{2\pi\hbar}{|E_{\overline{n}}'''|} \tag{23}$$

(with, for example, $E_{\overline{n}}'$ equal to the first derivative of energy E_n with respect to quantum number n, evaluated at $n=\overline{n}$) characterize the wave-packet's *classical motion*, *revivals*, and *super-revivals*, respectively. It is useful to connect these times with the Taylor series of the energy levels (centered at mean quantum number $\overline{n}$) by writing the latter in the form[25]

$$E_n=E_{\overline{n}}+2\pi\hbar\left[\frac{(n-\overline{n})}{T_1}\pm\frac{(n-\overline{n})^2}{T_2}\pm\frac{(n-\overline{n})^3}{T_3}\pm\cdots\right], \tag{24}$$

with the signs $\pm$ adjusted to ensure that times T_j are positive. The physical meaning of these time scales is shown by example in Sec. VI B.

A wave packet excited in the vicinity of mean quantum number $\overline{n}$ is associated with a corresponding mean scaled action $\alpha_{\overline{n}}$, via Eq. (10); a mean height ratio $\overline{r}=\alpha_{\overline{n}}/P$; and a mean energy $E_{\overline{n}}$, via Eq. (3). If we apply the general series solution to height ratio $r=\overline{r}$, we see that the expansion parameter η can be rewritten as

$$\eta=\frac{(n-\overline{n})\pi}{2}. \tag{25}$$

Thus Eq. (17) has the same form as the wave-packet expansion (24) and we can use it to extract expressions for the time scales. We find a classical motion time of

$$T_1=\frac{(1+P\sqrt{1-\overline{r}^2})}{P^2[\overline{r}\sqrt{1-\overline{r}^2}]}\frac{mL^2}{\hbar}; \tag{26}$$

a revival time of

$$T_2=\frac{4}{\pi}\frac{(1+P\sqrt{1-\overline{r}^2})^3}{P^2[(1-\overline{r}^2)(1+P\sqrt{1-\overline{r}^2})-\overline{r}^2]}\frac{mL^2}{\hbar}; \tag{27}$$

and a super-revival time of

$$T_3=\frac{24}{\pi^2}\frac{(1+P\sqrt{1-\overline{r}^2})^5}{P^2[\overline{r}P(4-\overline{r}^2)+4\overline{r}\sqrt{1-\overline{r}^2}]}\frac{mL^2}{\hbar}. \tag{28}$$

For a given wave packet, the connection between $\overline{n}$ and $\overline{r}$ is found by solving the transcendental equation (10) numerically, and then the wave-packet time scales are analytic functions of this numerical value of $\overline{r}$.

B. Example of wave-packet dynamics

Venugopalan and Agarwal[26] recently presented a numerical study of dynamics in finite square wells. With the expressions for the time scales, Eqs. (26)–(28), we complement their work with an analytic description of the dynamics. In this section, we give one example of wave-packet dynamics and make connections with the revival phenomena seen in other quantum potentials; a more detailed discussion of this work is presented elsewhere.[27]

We consider a Gaussian-shaped wave packet excited in a well of strength $P=100$. Initially the packet is in the center of the well, $\langle\hat{x}\rangle=0$, with width $\sqrt{\langle\hat{x}^2\rangle-\langle\hat{x}\rangle^2}=L/10$ and momentum $\langle\hat{p}_x\rangle=50\pi\hbar/L$. This wave packet is a superposition of approximately 20 energy levels centered around $\overline{n}=51$, excited in a well with 64 bound states. The height ratio associated with this state is $\overline{r}\approx 0.791\,97$, and the wave-packet time scales are $T_1\approx 0.0128mL^2/\hbar$, $T_2\approx 105.3T_1$, and $T_3\approx 615.3T_2$.

1. Classical motion

Initially this wave packet travels back and forth inside the well, moving as a localized entity and reflecting at the

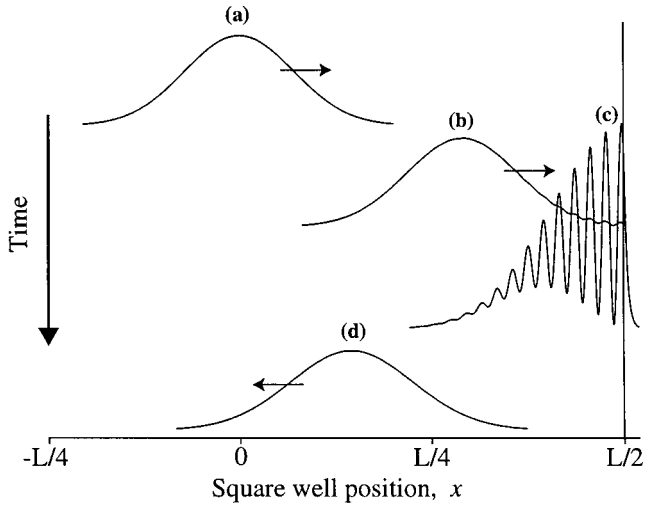

Fig. 1. Classical motion: Probability density $|\psi(x,t)|^2$ of a Gaussian wave packet shown at times (a) $0T_1$, (b) $T_1/7$, (c) $2T_1/7$, and (d) $3T_1/7$. In the first several periods of classical motion, the wave packet moves back and forth inside the square well, reflecting at the boundaries.

square-well boundaries (Fig. 1). The round-trip time for the wave packet is described by the classical motion time scale T_1. As the packet continues its motion, it begins to spread. By the fourth round trip, the wave packet has spread out entirely over the length of the square well (Fig. 2) and the periodic dynamics has decayed away.

The energy levels of the simple harmonic oscillator potential are equally spaced, $E_n=(n+1/2)\hbar\omega$. Wave packets excited in the harmonic oscillator have a classical period $T_1=2\pi/\omega$, but lack higher-order time scales ($T_2\rightarrow\infty$, $T_3\rightarrow\infty$, etc.). Thus all harmonic-oscillator wave packets have exact periodic motion[9] which lasts indefinitely. In contrast, we see that in the finite square well (as in other quantum systems with energy levels that are not equally spaced), classical motion is only observed in highly excited wave packets and survives only for a small window of time before decaying away.

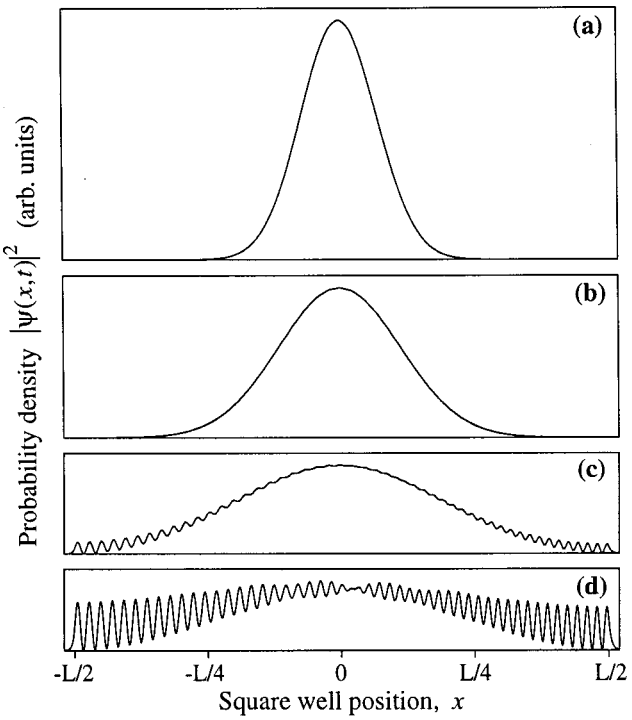

Fig. 2. Spreading: Probability density $|\psi(x,t)|^2$ of a Gaussian wave packet shown at times (a) $0T_1$, (b) $1T_1$, (c) $2T_1$, and (d) $3T_1$. The wave packet spreads during its periodic motion, and after four periods it has spread across the full length of the well.

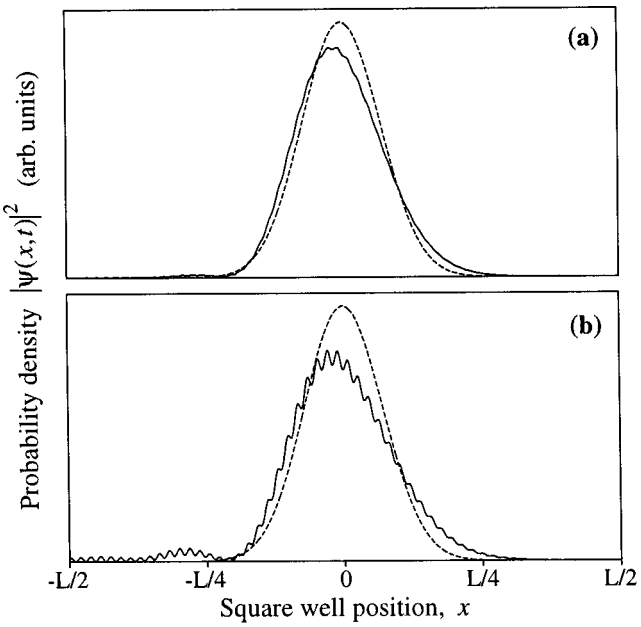

Fig. 3. Revivals: Probability density $|\psi(x,t)|^2$ of a Gaussian wave packet shown in the vicinity of times (a) $T_2/2$ and (b) T_2. During these revivals, the wave-packet shape and motion resurface for several classical periods. The light dashed lines show the original wave-packet shape.

2. Revivals

The shape and periodic dynamics of the wave packet resurface in windows of time called *revivals*, which occur[28] at multiples of time $T_2/2$ (for this wave packet, at multiples of approximately 52 classical periods). Figure 3 shows the wave packet during its first and second revivals, and we see that the wave-packet shape largely has been reformed.

The energy levels of the *infinite* square-well potential vary quadratically with quantum number, $E_n=E_1n^2$. Wave packets excited in the infinite well have a classical period $T_1=2\pi\hbar/(2\bar{n}E_1)$ and a revival time $T_2=2\pi\hbar/E_1$, but lack super-revival and higher-order time scales ($T_3\rightarrow\infty$, etc.). This leads to periodic motion (with period T_2) and mathematically exact full[9] and fractional[11] revivals of wave packets excited in the infinite well. In the finite well, the periodicity of the dynamics and the exactness of the revivals are broken by the finite potential depth.[26]

3. Super-revivals

Just as the shape of the wave packet slowly decays with each classical period, the quality of the wave-packet reformation decays with each revival [as can be seen by comparing Figs. 3(a) and (b)]. At much longer times, the wave-packet shape and periodic dynamics again re-surface in windows of time called *super-revivals*, which occur at multiples of time $T_3/6$ (for this wave packet, at multiples of approximately 10 800 classical periods). In Fig. 4, we see

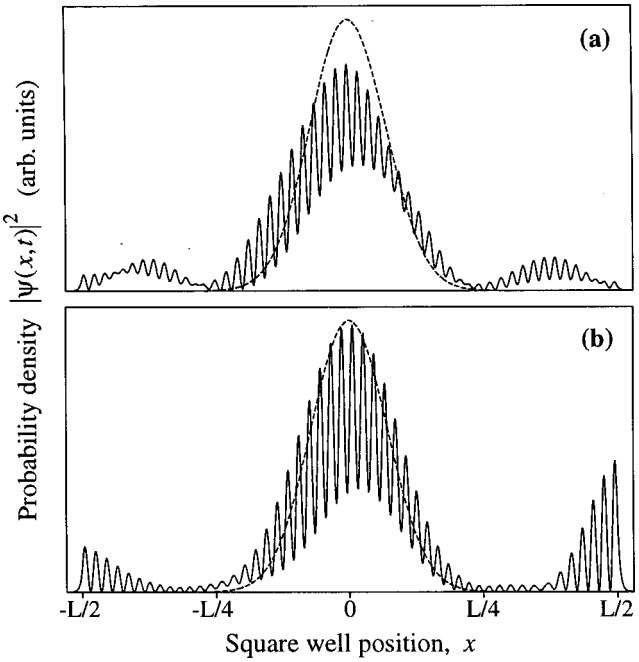

Fig. 4. Super-revivals: Probability density $|\psi(x,t)|^2$ of a Gaussian wave packet shown in the vicinity of times (a) $T_3/6$ and (b) $T_3/3$. During these super-revivals, the wave-packet shape and motion resurface for several revival periods. The light dashed lines show the original wave-packet shape.

that at the super-revivals the wave packet broadly has regained its original shape, but a noticeable fraction of the wave packet revives with opposite momentum (lagging behind the main packet by half a classical period), and the interference between left- and right-traveling momenta causes prominent ripples in the probability density.

We see that there are rather poor super-revivals for wave packets in the finite square well. This is quite different than for Rydberg atomic-electron wave packets, in which the initial wave-packet shape is better replicated during the super-revivals than at the revivals.[29]

ACKNOWLEDGMENTS

We thank Jake Bromage and Scott Walck for their discussions and feedback on this manuscript. This work was partially supported by the GAANN program of the U.S. Department of Education and by the Army Research Office through the MURI Center for Quantum Information.

[a]Electronic mail: daron@optics.rochester.edu

[1]C. D. Cantrell, ''Bound-state energies of a particle in a finite square well: An improved graphical solution,'' Am. J. Phys. **39**, 107–110 (1971).
[2]S. Gasiorowicz, *Quantum Physics* (Wiley, New York, 1996), 2nd ed., pp. 78–83.
[3]D. J. Griffiths, *Introduction to Quantum Mechanics* (Prentice–Hall, Englewood Cliffs, NJ, 1995), pp. 60–66.
[4]R. L. Liboff, *Introductory Quantum Mechanics* (Addison–Wesley, Reading, MA, 1992), 2nd ed., pp. 275–284.
[5]H. C. Ohanian, *Principles of Quantum Mechanics* (Prentice–Hall, Englewood Cliffs, NJ, 1990), pp. 78–84.
[6]For an introductory discussion of wave-packet dynamics in the hydrogen atom and its connections to classical mechanics, see M. Nauenberg, C. R. Stroud, Jr., and J. Yeazell, ''The classical limit of an atom,'' Sci. Am. **270**, 24–29 (June 1994).
[7]J. Parker and C. R. Stroud, Jr., ''Coherence and decay of Rydberg wave packets,'' Phys. Rev. Lett. **56**, 716 (1986).
[8]M. Nauenberg, ''Autocorrelation function and quantum recurrence of wavepackets,'' J. Phys. B **23**, L385–L390 (1990).
[9]R. Bluhm, V. A. Kostelecký, and J. A. Porter, ''The evolution and revival structure of localized quantum wave packets,'' Am. J. Phys. **64**, 944–953 (1996).
[10]Z. D. Gaeta and C. R. Stroud, Jr., ''Classical and quantum-mechanical dynamics of a quasi-classical state of the hydrogen atom,'' Phys. Rev. A **42**, 6308–6313 (1990).
[11]D. L. Aronstein and C. R. Stroud, Jr., ''Fractional wave-function revivals in the infinite square well,'' Phys. Rev. A **55**, 4526–4537 (1997).
[12]B. I. Barker, G. H. Rayborn, J. W. Ioup, and G. E. Ioup, ''Approximating the finite square well with an infinite well: Energies and eigenfunctions,'' Am. J. Phys. **59**, 1038–1042 (1991).
[13]L. I. Schiff, *Quantum Mechanics* (McGraw–Hill, New York, 1968), 3rd ed., pp. 37–44.
[14]P. H. Pitkanen, ''Rectangular potential well problem in quantum mechanics,'' Am. J. Phys. **23**, 111–113 (1955).
[15]P. G. Guest, ''Graphical solutions for the square well,'' Am. J. Phys. **40**, 1175–1176 (1972).
[16]R. D. Murphy and J. M. Phillips, ''Bound-state eigenvalues of the square-well potential,'' Am. J. Phys. **44**, 574–576 (1976).
[17]W. C. Elmore, ''Eigenvalues of the square-well problem,'' Am. J. Phys. **39**, 976–977 (1971).
[18]E. J. Burge, ''Improved simple graphical solution for the eigenvalues of the finite square well potential,'' Eur. J. Phys. **6**, 154–164 (1985).
[19]B. C. Reed, ''A single equation for finite rectangular well energy eigenvalues,'' Am. J. Phys. **58**, 503–504 (1990). We note that Pitkanen (Ref. 14) mentioned the possibility of such a unified equation, without developing it analytically, some 35 years earlier.
[20]D. W. L. Sprung, H. Wu, and J. Martorell, ''A new look at the square well potential,'' Eur. J. Phys. **13**, 21–25 (1992).
[21]P. M. Morse and H. Feshbach, *Methods of Theoretical Physics* (McGraw–Hill, New York, 1953), Vol. 1, pp. 411–413.
[22]M. Abramowitz and I. A. Stegun, *Handbook of Mathematical Functions* (Dover, New York, 1972), p. 16.
[23]D. W. L. Sprung, H. Wu, and J. Martorell, ''Poles, bound states, and resonances illustrated by the square well potential,'' Am. J. Phys. **64**, 136–144 (1996).
[24]W. H. Press, S. A. Teukolsky, W. T. Vetterling, and B. P. Flannery, *Numerical Recipes: The Art of Scientific Computing* (Cambridge U.P., Cambridge, 1992), 2nd ed., Sec. 9.4. Note also that numerical iteration methods for finding energy levels are discussed in detail by Murphy and Phillips (Ref. 16).
[25]C. Leichtle, I. Sh. Averbukh, and W. P. Schleich, ''Multilevel quantum beats: An analytical approach,'' Phys. Rev. A **54**, 5299–5312 (1996).
[26]A. Venugopalan and G. S. Agarwal, ''Superrevivals in the quantum dynamics of a particle confined in a finite square-well potential,'' Phys. Rev. A **59**, 1413–1422 (1999).
[27]D. L. Aronstein and C. R. Stroud, Jr., ''Analytical investigation of revival phenomena in the finite square-well potential,'' Phys. Rev. A **62**, 022102 (2000).
[28]The first wave-packet revival occurs in the vicinity of time $T_2/2$, but the exact moment when the re-formed packet passes through its original location is a (known) function of both T_1 and T_2. Similarly, the details of super-revival phenomena depend on T_1, T_2, and T_3. This is discussed on O. Knospe and R. Schmidt, ''Revivals of wave packets: General theory and applications to Rydberg clusters,'' Phys. Rev. A **54**, 1154–1160 (1996).
[29]R. Bluhm and V. A. Kostelecký, ''Long-term evolution and revival structure of Rydberg wave packets,'' Phys. Lett. A **200**, 308–313 (1995).